Received: 12 October 2020 | Revised: 5 February 2021 | Accepted: 9 February 2021

DOI: 10.1111/jfpp.15352

ORIGINAL ARTICLE

Journal of Food Processing and Preservation Institute of Food Science + Technology ifst WILEY

Semolina extraction from wheat bran using an electro-separation process

Messaouda Kahaleras | Mokdad Remadnia | Miloud Kachi | Abdelkader Nadjem

Electrical Engineering Laboratory – LGEG, University 8 May 1945, Algeria

Correspondence
Kachi Miloud, Electrical Engineering Laboratory – LGEG, University 8 May 1945, B.P.401, Guelma 24000, Algeria.
Email: kachi.m@univ-guelma.dz

Abstract

The present paper is aimed at studying the improvement of the semolina extraction from durum wheat grains through a recycling of wheat bran, as a by-product, issued from traditional milling and sieving. Abrasion of the wheat bran and then electrostatically separating obtained components allowed a recovery of a significant amount of semolina, reaching 50% of the treated mass. Three components were obtained after separation, namely, semolina, fine bran, and relatively big bran. The electrostatic characterization, including surface potential decay and charge measurement, showed a clear conductive character with a slight difference between components in terms of charge conservation. This electric conductive behavior of the wheat bran leads to choose an induction-type electrostatic separator to extract residual semolina from the grinding process. The design of experiments methodology was used to study the influence of the main parameters: the applied high voltage, the conveyor speed, and the speed of the rotating part. The process was optimized taking into consideration both the quantity and quality of the recovered semolina, targeting a high recovery rate with the best possible quality. The physical and chemical analysis showed a good quality of the recovered semolina with 1.1% ash content.

Practical applications

The wheat milling process in an industrial installation passes through several steps that are optimized to extract maximum semolina from grains. However, still a residual endosperm stays attached to the bran due to the process itself. Literature estimates wheat bran around 15% of the grain, which can be an important quantity taking into account the huge amount of cereal produced and consumed around the world. The suggested complementary process aims at the extraction of residual semolina attached to wheat bran through treating wheat bran by abrasion and later separate obtained components using and an electrostatic field. Obtained results, showed that treating wheat bran using the suggested method allows recovery of around 50% as semolina from the treated quantity. So, this reduces thrown wheat bran quantity to the half, which is important from an industrial point of view since it increases the production from the same wheat quantity.

1 | INTRODUCTION

Durum and common wheat are among the most important agricultural products, particularly used for human consumption because of their nutritive profile and relatively easy harvesting, storing, and processing, as compared to other grains (Hutkins Robert, 2019; Kulp, 2000). Wheat grain has a complex structure composed of distinct adhesive tissues (Surget & Barron, 2005). So, to achieve the physical disentanglement of individual components, grains are milled using, mainly, a mechanical process (Wang et al., 2014). The quality of the milling process is dependent on the distinct biomechanical properties of the wheat grain layers and their tissue-adhesive forces (Burton Rachel & Fincher Geoffrey, 2014; Hourston et al., 2017). The wheat milling process consists of the separation of the endosperm from the other parts of the kernel (i.e., bran and germ), and the reduction of the endosperm to semolina and then to flour. This operation involves the reduction of kernels into smaller particles that can be utilized and transferred into palatable products (Samaan, 2007). Wheat bran is considered as a by-product of the milling process, which serves as a livestock feed in most cases while only a fraction is used in the food industry (Hossain et al. 2013; Onipe et al., 2015). The conventional milling process is realized through grinding grain between two rotating cylinders. This mechanical process is far from being a perfect operation. The mechanically separated wheat bran still contains residues of the endosperm part (white parts in Figure 1). Besides, during the sieving stage semolina, or flour, particles can stay attached to the bran. The bran represents 15% of the wheat grain (Hill, 2014). If losses due to milling imperfections are also considered, the thrown quantity of wheat bran can be important relative to the initial mass of wheat grains. So, given the huge quantities of produced wheat, this rate of bran can be considered as a wasting of such an important product. Electrostatic separation has emerged as a novel process for dry food ingredient fractionation and mineral enrichment (Kdidi et al., 2019; Rajaonarivony et al., 2017; Wang et al., 2015). It was especially employed when particles have different electrical and/or physical properties (Wang et al. 2014) The electrostatic separation allowed the production of purified fractions from wheat bran, exhibiting very different particle structure and composition: fractions rich in aleurone or rich in the most outer layers were produced (Hemery et al., 2011). Combination of proper mechanical milling and electrostatic separation is a promising technology for sorting plant and agro-resources (Barakat & Mayer-Laigle, 2017; Laguna et al., 2018).

This paper is aimed at applying a combination of mechanical fractioning and electrostatic separation to increase the recovery of semolina particles from durum wheat bran after the milling process. The proposed step is a complementary procedure to traditional sieving allowing, however, an increase in the extraction rate of semolina, without affecting product quality and taking advantage of low energy consumption of the electrostatic separators.

2 | EXPERIMENTAL PROCEDURE

2.1 | Samples preparation

The experiments were performed on samples of durum wheat bran provided by a local food company (Amor Benamor Group, El Fedjoudj-Guelma, Algeria). The wheat bran samples were produced from the grains harvested in the east of Algeria using a conventional milling process. During this study, sample preparation is a first and crucial step in the proposed procedure. Preparation consists of mechanically detaching the white residuals from the internal face of the wheat bran through an abrasive process. The abrasive device used throughout the experiments is shown in Figure 2. It is mainly composed of two horizontally aligned disks separated by a distance of 20 mm. The fixed lower disk contains a metallic grid mounted on an aluminum disk. The upper disk is driven by an electric motor at a variable speed (Max speed = 1,300 rpm). The wheat bran is introduced in the abrasion chamber from a hopper feeder. The minimum gap between the abrasive surface and the metallic grid can be adjusted manually through a distance adjusting arm. When abrasion is over, the new fraction of the mixture was collected in a wooden box attached to the abrasion chamber, then, packaged in a polyethylene bag before passing to the next step. The prepared wheat bran is then transferred to the electrostatic separator to be purified.

All the experiments were carried out in an ambient air at 22 ± 1°C and relative humidity 38% ± 1%. Virgin samples were employed for each test.

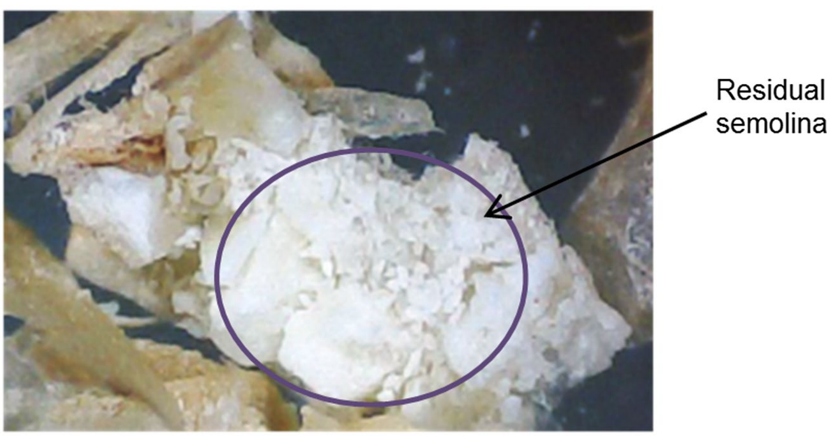

FIGURE 1 Microscope image (magnification: 60×) of wheat bran recovered after the traditional milling process

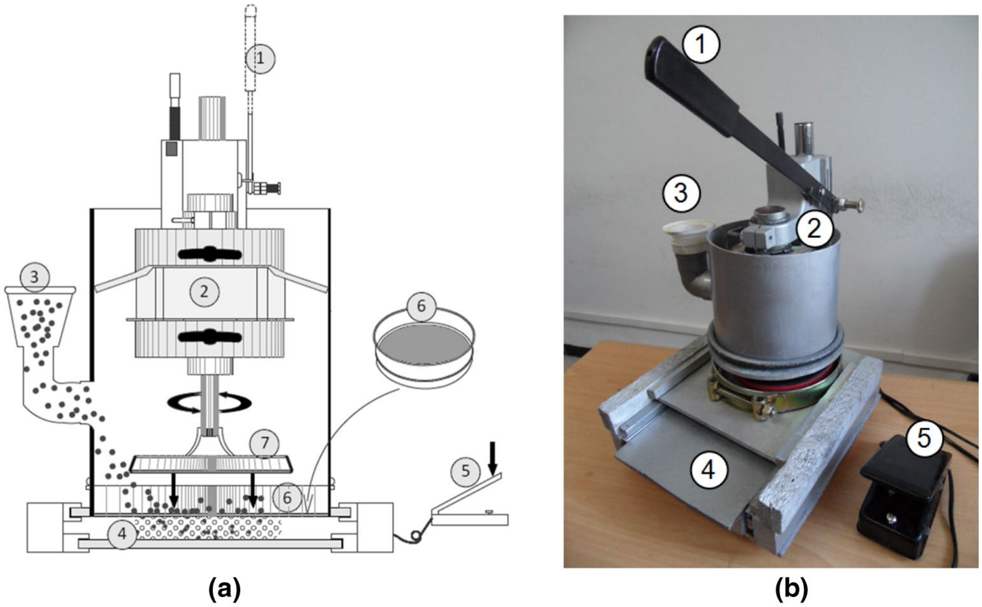

FIGURE 2 Wheat bran abrasion device: (a) Schematic representation, (b) Photography of the laboratory device for wheat bran abrasion (1: inter-disk distance adjusting arm, 2: electric motor, 3: hoper, 4: collecting box, 5: disk speed controller, 6: metallic grid, 7: rotating disk)

2.2 | Electrostatic separation experiments

The lab prepared roll-type electrostatic separator is shown in Figure 3. The separator uses electrostatic induction as a mechanism to separate components, in this case, semolina particles from the external brown layer. Through the vibratory feeder, the mixed material, consisting of prepared wheat bran, is dispersed as a monolayer on the surface of a moveable grounded plate electrode driven by a variable speed electric motor. The dispersed material is transported toward the rotating roll at a 44 cm distance between the deposition point and the separation region. A rotating stainless steel roll (diameter: 13 cm; length: 14.5 cm) suspended at 2 cm height from the moveable grounded plate is connected to a positive high-voltage power supply (Model: FuG Elektronik GmbH 83024 Rosenheim/Germany). A high-intensity electric field is generated between this rotating electrode and the grounded metallic plate electrode. As the prepared bran sample crosses the electric field, the finest particles are charged by electrostatic induction and rapidly attracted by the roll electrode, having an opposite polarity. Most of these fine particles stay on the roll surface until arriving at the collecting box (1), where they can be detached by a scraper. The relatively large brown particles coming from the outer side of the bran are also attracted by the roll. Because of centrifugal forces, these particles fall at a certain height. The second collecting box (2) is installed exactly where these large particles fall in a way to prevent their returning to the grounded plate. Semolina particles are unaffected by the electric field and, therefore, they stay on the grounded plate electrode and collected in the box (3). The separation efficiency of wheat bran depends on the applied high voltage U, the rotation speed of the roll electrode n, and the conveyer speed v. The effects of these three factors on the outcome of the separation are evaluated using the experimental design methodology. With such a technique, all the relevant factors of the process are varied simultaneously over a set of planned experiments. The results are connected by a mathematical model. In the present study, the objective will be to improve the efficiency of the multifactorial electrostatic separation process and to increase the purity of the recovered semolina fraction.

2.3 | Electrostatic characterization of wheat bran components

2.3.1 | Surface potential decay experiments

Surface potential decay measurements provide a useful tool to gauge electrical properties of materials under study when in contact with a grounded electrode, after being exposed to a corona discharge (Kachi et al., 2011; Remadnia et al., ,2011, 2014). The SPD experiments were performed on the three collected products in the collecting boxes of the electrostatic separator. They were dispersed as mono-layered samples for each material. The samples were located on a grounded metallic plate (length: 13 cm and width: 11 cm). The open side of the sample was subjected to a corona discharge for 10 s, using a high-voltage needle electrode (diameter: 100 μm). The distance between the needle electrode and the surface of the grounded plate electrode was 20 mm. The surface potential was then monitored using a Monroe probe placed above the sample surface and positioned right in the middle. The probe was connected to an electrostatic voltmeter (Trek model 347), driven by a personal computer. The acquisition and processing of the experimental data was performed using a

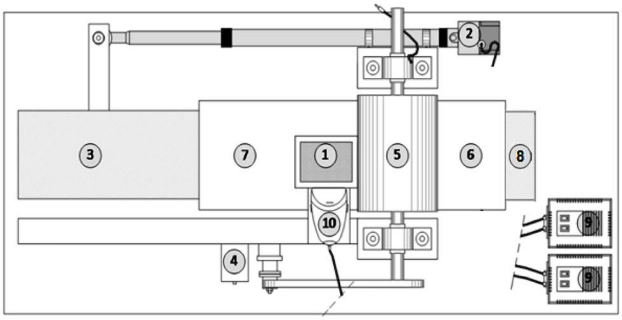

(a)

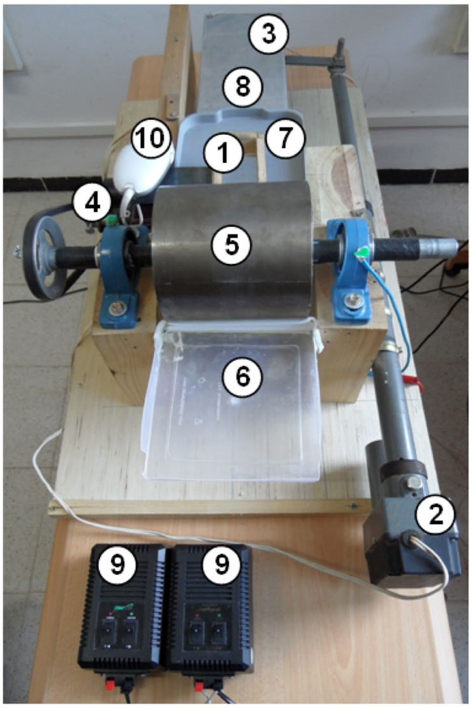

(b)

FIGURE 3 Roll-type electrostatic separator: (a) Schematic representation of the roll-type electrostatic separator, (b) Photography of the electrostatic separator of wheat bran powder (1: feeder, 2: linear actuator, 3: grounded plate electrode, 4: driving motor, 5: rotating roll electrode, 6: collecting box 1, 7: collecting box 2, 8: collecting box 3, 9: manual electric control, 10: vibratory device)

custom-designed virtual instrument, developed in DASYLab environment. When corona charging is turned off, the base wooden turns 180 degrees for positioning the probe above the sample for measuring surface potential (Figure 4).

2.3.2 | Charge measurements

The electric charge was measured using a sensitive electrometer (Keithley model 6514) and a Faraday pail-type collecting box (Chubb, 2010). As soon as the separation is over, the separated products are directly poured in the Faraday pail for charge measurement. Afterward, the samples are weighted using an electronic balance of 0.01 g resolution. In this way, the electric charge can be expressed in terms of the charge/mass ratio (nC/g) for each product.

2.4 | Experimental design methodology

As the objective was the modeling and optimization of the separation process, face-centered central composite design, based on quadratic polynomials models, is generally used (Eriksson et al., 2008; Frigon & Mathews, 1996). With such models, the process response is expressed as a function of factors u_i ($i = 1, \ldots, e$):

$$y = f(u_i) = c_o + \sum c_i u_i + \sum c_{ij} u_i u_j + \sum c_{ii} u_i^2 \qquad (1)$$

A normalized centered value can be defined for each factor as follows:

$$x_i = (u_i - u_{ic}) / \Delta u_i = i_i^* \qquad (2)$$

where:

$$u_{ic} = (u_{i\,max} + u_{i\,min}) / 2 \qquad (3)$$

$$\Delta u_i = (u_{i\,max} - u_i\, min) / 2 \qquad (4)$$

With these notations, the response function becomes:

$$y = f(x_i) = a_0 + \sum a_i x_i + \sum a_{ij} x_i x_j + \sum a_{ii} x_i^2 \qquad (5)$$

For the factors that have been considered in the present study, that is, the positive high-voltage level U (kV, the roll speed n (rpm), and the conveyor speed v(cm/s), the quadratic model of the response y, that is, the mass collected in each box, will take the following form:

$$y = a_0 + a_1 U^* + a_2 n^* + a_3 v^* + a_{12} U^* n^* + a_{13} U^* v^* + a_{23} n^* v^* + a_{11} U^{*2} + a_{22} n^{*2} + a_{33} v^{*2} \qquad (6)$$

The results were processed in MODDE 8.0 software (Umetrics, 2006).

2.5 | Moisture, ash, and yellow pigment content analysis

After the electrostatic separations experiments, the obtained samples of semolina were analyzed for moisture, ash, and yellow

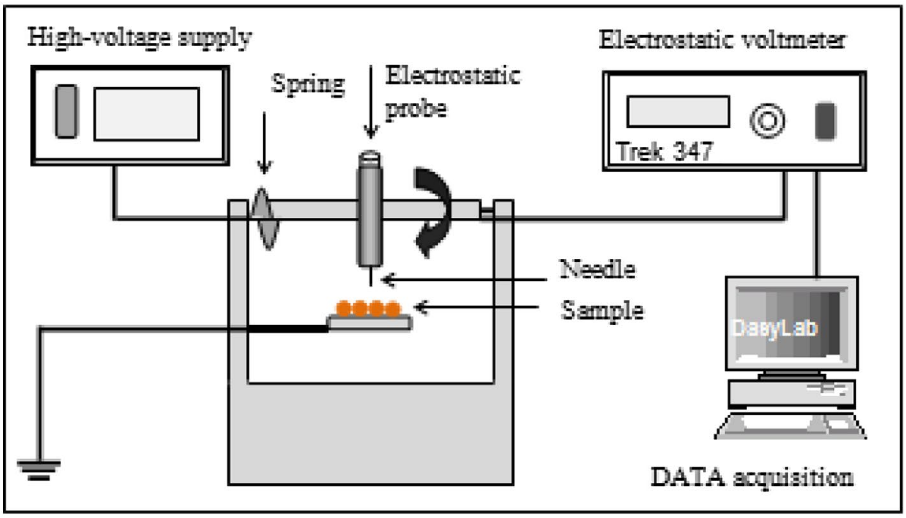

FIGURE 4 Experimental setup for surface potential decay measurements

FIGURE 5 Wheat bran microscopic images (a) before and (b) after abrasion process (magnification: 60×)

pigment content. Each analysis was repeated three times and results are given in terms of mean values with a standard deviation below 5%. Granulometry measurement was performed according to the norm AFNOR NF 03-721.

3 | RESULTS AND DISCUSSION

3.1 | Wheat bran milling results

Figure 5 shows microscope images of wheat bran particles before and after abrasion. Untreated wheat bran particles (Figure 5a) contain large pieces of bran with considerable amounts endosperms still adhering to the bran layers before processing. Figure 5b shows a microscope picture of ground material with the abrasive device. The coarse bran reveals a bran area in which the cell wall is removed, leaving the outline of their attachment to the aleurone layer.

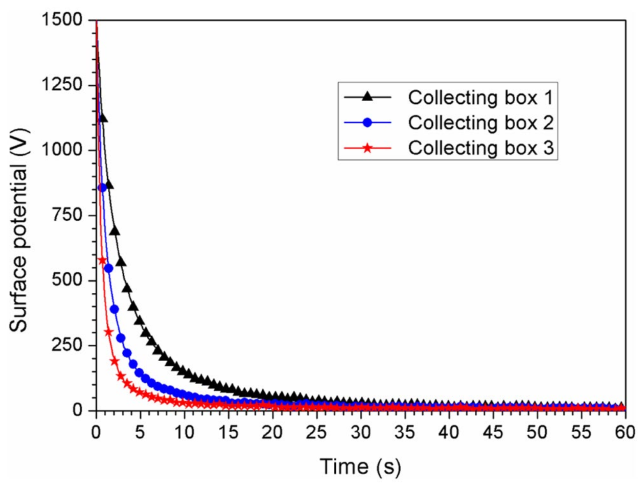

FIGURE 6 Surface potential decay curves recorded for $t = 60$ s after corona charging the fractions of fine wheat bran (box 1), wheat bran (box 2), and semolina (box 3). The curves are the average of at least three runs. (standard deviation < 50V)

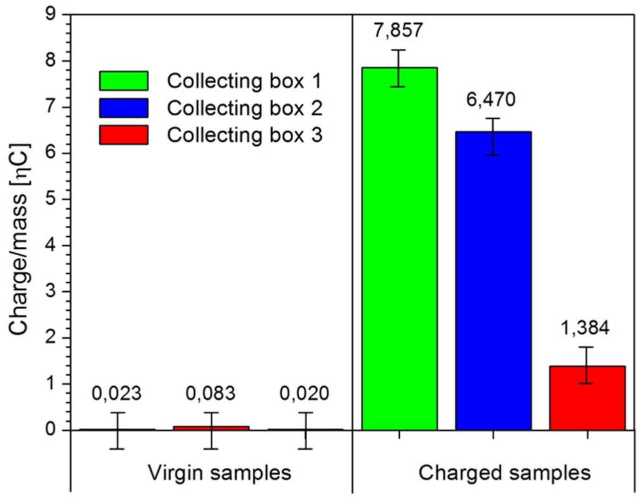

FIGURE 7 Charge per mass ratio of bran fine fraction, bran fraction, and semolina fraction before and after separation, $U = 10.5$ kV, $n = 28$ rpm and $v = 0.5$ cm/s (the results are averages of three runs)

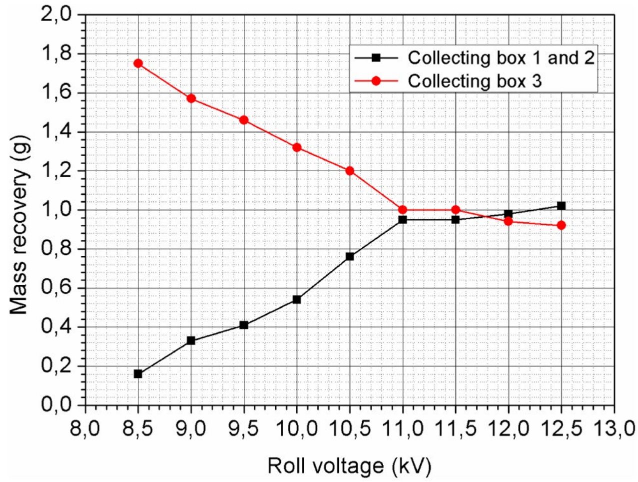

FIGURE 8 Recovery of products as function of the roll voltage ($m_0 = 2$ g; T = 22°C ± 1; RH = 38% ±1; $n = 28$ rpm; $v = 0.5$ cm/s)

3.2 | Electrostatic characterization of wheat bran components

3.2.1 | Surface potential decay

The surface potential decay experiments were carried out after electrostatic separation. Figure 6 displays a set of SPD curves under the same electric field for the recovered fractions in the collecting boxes 1, 2, and 3. The decay of the potential at the surface of the semolina fraction layer recovered in box 3 is faster than that for bran fractions collected in boxes 1 and 2. Indeed, during the first 10 s after corona charging, the absolute value of the surface potential of semolina fraction diminishes by more than 97%, from 1.52 kV to 0.032 kV. Under similar experimental conditions, the potential at the surface of layers composed of bran particles diminishes by 90% from 1.52 kV to 0.148 kV. A similar reduction is observed with bran fine fraction collected in box 1. During the 30 s, the three fractions lose completely their electric charge. This means that the studied particles behave as bad insulators, and do not conserve the electric charge for a long time. This conductive behavior justifies the choice of induction mechanism to carry electrostatic separation.

3.2.2 | Charging state characterization

The charge measurements were carried out before (virgin samples) and after separation (charged samples). The charge/masse ratios recorded for the three fractions (i.e., fine bran, bran, and semolina) are shown in Figure 7. The measurements after separation were carried out for samples with initial mass $m_0 = 2$ g, the roll voltage is set at $U = 10.5$ kV, the plate speed is fixed at $v = 0.5$ cm/s while the rotating roll speed at $n = 28$ rpm. Before corona charging, the average value of the residual charge of virgin samples is 0.04 ηC/g. In the case of semolina fraction, the recorded charge/mass ratio after separation is very low (1.38 ηC/g). These measurements confirm once again the conductive behavior of semolina fraction. Consequently, these electrically conductive particles lose their acquired charge through the grounded plate electrode. On the contrary, the value of the acquired charge measured for the fractions of bran and fine bran is relatively important (6.47 ηC/g and 7.85 ηC/g, respectively). The wheat bran samples are slightly more resistive than the semolina samples, which allow them to keep some of the acquired charge. Further, the flat elongated shape of wheat bran particles provides a larger contact with the plate electrodes, and hence, favors their charging by conductive induction.

3.3 | Effect of the roll voltage on the recovery results

The collected quantities in the three boxes are weighted with an electronic balance. The recorded values for the two boxes 2 and 3 are summed up to obtain the total mass of the attracted products by the roll electrode. The material losses for these experiments are very low, representing less than 5% of the feed. The variations of recovered mass in the collecting box 3 and the sum of masses recovered in boxes 1 and 2 as a function of the roll voltage are presented in Figure 8. The plate speed was fixed at $v = 0.5$ cm/s and the rotating roll speed at $n = 28$ rpm, with ambient temperature and humidity 22°C ± 1 and 38% ± 1, respectively. The initial sample weight was $m_0 = 2$ g. The results presented in Figure 8 can be divided into three regions: (i) below 8.5 kV there is no significant separation, almost all the powder stays on the conveyer electrode, and recovered in the collecting box 3. (ii) From 8.5 kV up to 11 kV, the separation is increasingly enhanced, leading to

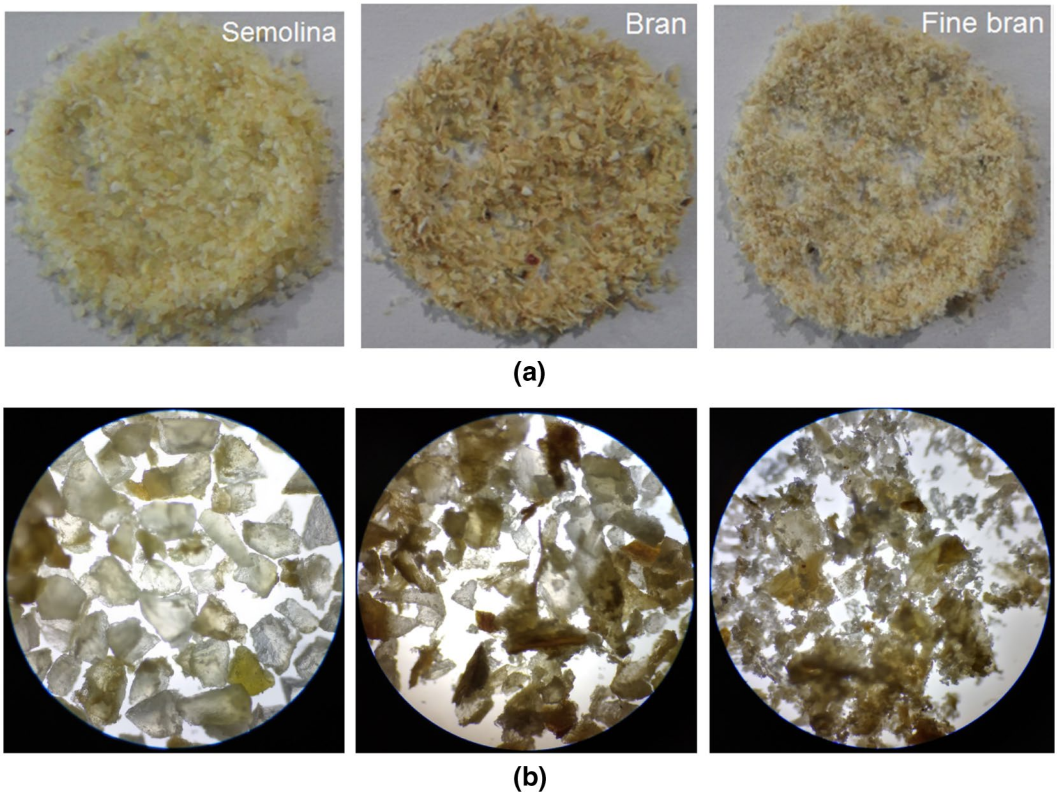

FIGURE 9 Fractions obtained: (a) image of fractions (b) Microscope images (magnification: 40×) of fractions obtained with an optical microscope (OPTIKA B–150)

particles attraction by the roll and their recovery in the collecting box 1. The rebounded particles and those detached by centrifugal force, after a contact with the roll electrode, were recovered in the collecting box 2. The rest of the powder stays on the plate and passes directly to the box 3. (iii) Between 11 kV and 12.5 kV, a kind stabilization is established resulting in equal quantity separation. The optimal voltage should be inspected in this voltage interval. The fractions collected in boxes 1 and 2 have very low density, both are characterized by flat elongated particles of brown color. The fraction collected in the box 3 is denser than the fraction collected in the box 1 and 2 and characterized by spherical particles of cream color. The difference noticed between fractions 1 and 2 is that the fraction collected in box 1 is very fine compared to the fraction recovered in box 2.

Figure 9 shows both real and microscope images of recovered materials in the three collecting boxes. Differences between the three materials are obvious, in terms of color and shape.

From Figure 9, it appears that the wheat semolina fraction recovered in box 3 is characterized by smooth surfaces without cracks. The size and shape of the semolina is very heterogeneous, and the particles have a size much higher than that of other wheat bran fractions recovered in boxes 1 and 2. A conducting particle in contact with the grounded plate when it enters the electric field gets charged by electrostatic induction. It can be attracted by the roll electrode, if the electric attraction force F_e exceeds both the gravitational force F_g and adhesion force F_a: $F_e > F_a + F_g$.

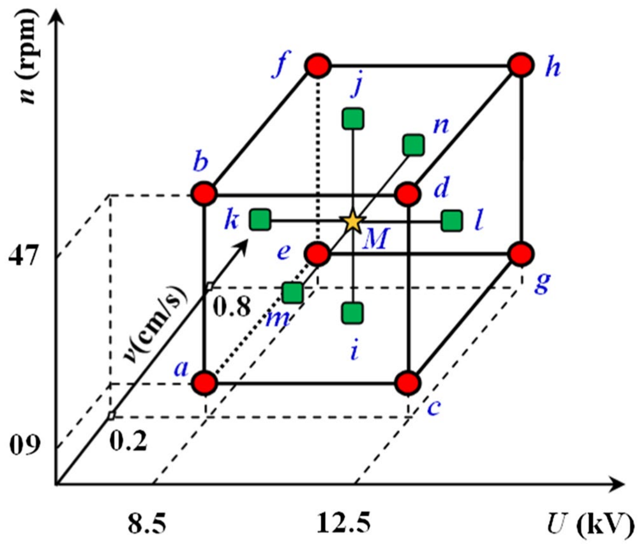

FIGURE 10 Diagram of experiments of a face centered central composite design (FCCD) with three factors: applied voltage U (U_{min} = 8.5 kV and U_{max} = 12.5 kV), roll speed n (n_{min} = 9 rpm and n_{max} = 47 rpm), and conveyer plate speed v (v_{min} = 0.2 cm/s and v_{max} = 0.8 cm/s)

TABLE 1 Results of the FCCD experimental design

Run No.	Factors U (kV)	n (rpm)	v (cm/s)	Responses $Y_{Box\ 1}$ (g)	$Y_{Box\ 2}$ (g)	$Y_{Box\ 3}$ (g)
1	8.5	9	0.2	0.04	0.02	1.92
2	12.5	9	0.2	0.58	0.47	0.9
3	8.5	47	0.2	0.09	0.03	1.83
4	12.5	47	0.2	0.99	0.71	0.28
5	8.5	9	0.8	0.01	0.02	1.91
6	12.5	9	0.8	0.4	0.7	0.88
7	8.5	47	0.8	0.01	0.03	1.93
8	12.5	47	0.8	0.67	0.94	0.36
9	8.5	28	0.5	0.04	0.02	1.9
10	12.5	28	0.5	0.69	0.6	0.65
11	10.5	9	0.5	0.19	0.05	1.71
12	10.5	47	0.5	0.38	0.1	1.47
13	10.5	28	0.2	0.4	0.2	1.39
14	10.5	28	0.8	0.22	0.32	1.41
15	10.5	28	0.5	0.3	0.17	1.51
16	10.5	28	0.5	0.31	0.15	1.52
17	10.5	28	0.5	0.31	0.14	1.53

It is important to optimize the different parameters of the process to increase its efficiency. This has been achieved using experimental design methodology as described in the last section.

3.4 | Face-centered central composite design (FCCD)

Based on the results of preliminary separation tests, three factors were considered as most influential for which we determine limits of variation:

- Roll voltage U: $U_{min} = 8.5$ kV and $U_{max} = 12.5$ kV;
- Plate speed v: $v_{min} = 0.2$ cm/s and $v_{max} = 0.8$ cm/s;
- Roll speed n: $n_{min} = 9$ rpm and $n_{max} = 47$ rpm.

The output variables of the system are masses of recovered materials in the tree boxes. Figure 10 shows experiments of a face-centered central composite design allowing the use of Response Surfaces Modeling (RSM). It consists of eight experiments located at the cube's corners (round points *a*, *b*,…, *h*), six experiments located at the centers of the cube faces (square points *i*, *j*,…, *n*) and three identical experiments done at the central point, *M* (star point). The results of 17 experiments of the FCCD experimental design carried out with 2 g of ground wheat bran samples are given in Table 1. The following mathematical models are obtained for the recovered powders masses:

$$Y_{box1} = 0.306 + 0.314U^* + 0.092n^* - 0.079v^* + 0.059U^2 + 0.078U^*n^* - 0.048U^*v^* - 0.023n^*v^* \quad (7)$$

$$Y_{box2} = 0.147 + 0.330U^* + 0.055n^* - 0.058v^* + 0.167U^{*2} - 0.067n^2 + 0.117v^{*2} + 0.057U^*n^* + 0.057U^*v^* \quad (8)$$

$$Y_{box3} = 1.514 - 0.642U^* - 0.145n^* - 0.016v^* - 0.234U^{*2} + 0.080n^{*2} - 0.109v^{*2} - 0.133U^*n^* + 0.026n^*v^* \quad (9)$$

The descriptive and predictive capabilities of the three models, expressed respectively by the statistic coefficients R^2 and Q^2. The goodness of fit coefficient R^2 is close to 1 for the three models, 0.997, 0.989, and 0.999, respectively, which means that the recovered masses are well described by the quadratic polynomials (7), (8), and (9). The goodness of prediction coefficients Q^2 of the three models is also rather elevated: 0.976, 0.963, and 0.996, respectively. The values of the coefficients associated with the factors in the mathematical model show the degree of influence of each factor. The coefficients are also plotted in Figure 11. The statistical analysis of the data, using Student's *t* test, indicates that the effects of all factors (i.e., the coefficients of U^*, v^*, and n^*) are significant. The coefficients of n^{*2} and v^{*2} in the first model, n^*v^* in the second model, and U^*v^* in the third model are not statistically significant, they were removed from the $Y_{box\ 1}$, $Y_{box\ 2}$, and $Y_{box\ 3}$. The models shows that the most influential parameter on the recovered masses is the high voltage (coefficients = 0.314, 0.330, and −0.642), followed by the roll speed (coefficients = 0.092, 0.055, and −0.145), and then, the conveyer plate speed (coefficients= −0.079, 0.058, and 0.016).

The influence of each factor on the three responses (mass collected in box 1, box 2, and box 3) is shown in Figure 12. The iso-response curve calculated with the model of the recovered mass in collecting box 3 is represented in Figure 13, within the domain of the three factors. Quite surprisingly, the effects of the factors considered in the present study seem to be different on the three sorts of recovered materials. Without any doubt, the applied voltage U has a stronger effect on the recovered masses in the three collecting boxes. Indeed, with the increase of the voltage applied to the rotating roll, the mass collected in box 1 and box 2 increases, and that in box 3 decreases. The higher is voltage U the stronger is the electric field forces acting on the particles, leading to larger recovered masses. Similarly, the rotation speed of the roll n also demonstrated perceptible influences on the three responses. The increase of the roll speed results in an increase of centrifugal force and a reduction of residence time of attached particles to the roll. This explains the increase of collection in boxes 1 and 2. The speed of the conveyer plate electrode v seems to have little influence compared to the other parameters. The faster the plate moves, the shorter is the time the particle stays in the electric field and the less is the charge they can acquire. Therefore, insufficiently charged particles will not be attracted to the rotating electrode and remains on the plate electrode. According to the data analysis performed with MODDE 8.0, there exists a strong interaction between the roll voltage U and the roll speed n: at lower applied voltage U, the modification of the roll speed has only a marginal

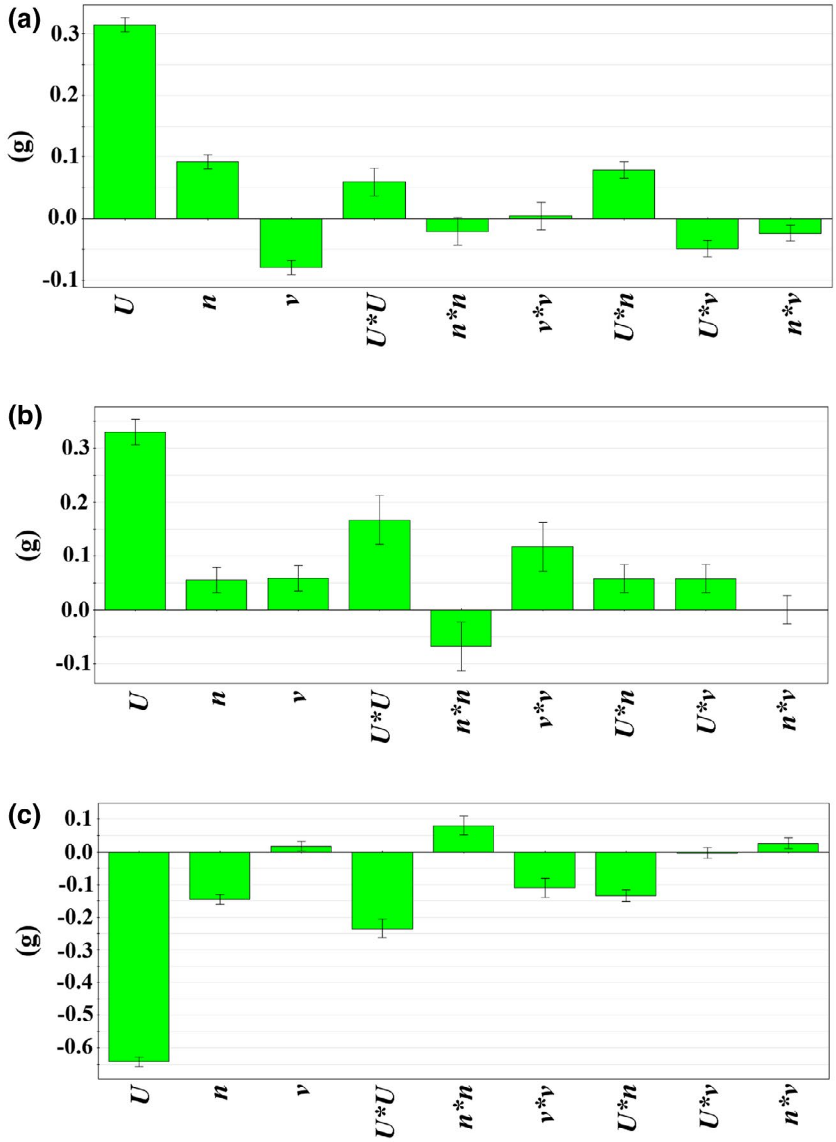

FIGURE 11 MODDE 8.0-computed coefficients of the quadratic polynomial models for recovered mass in box 1 (a), box 2 (b), and box 3 (c)

effect on the recovered masses in the collecting boxes as can easily be seen in Figure 13.

To ensure the increase of the purity and the recovery rate of semolina, systematic experiments of electrostatic separation and semolina fraction quality control tests are necessary to correlate the best settings of control variables of the process and the purity characteristics of the product obtained after separation. The optimization stage of this experimental process should allow the determination of factors values for which the recovered mass in box 3 is close to a target. For an initial weight of 2 g, the established model $Y_{\text{box }3}$ indicates that optimum operating conditions (i.e., the target: $Y_{\text{Box3}} = 1$ g, predicted mass in box 1 is 0.54 g and predicted mass in box 2 is 0.42 g) correspond to a roll voltage $U = 12.4$ kV, roll speed $n = 9.73$ rpm, and a conveyer plate speed $n = 0.34$ cm/s. A verification experiment conducted by application of obtained optimal values leads to the following results: 0.98 g in box 3 (semolina), 0.53 g in box 1 (bran), and 0.41 g in box 2 (fine bran), which confirms the predictions made by MODDE 8.0.

3.5 | Physical and chemical analysis

The results of the physical and chemical analysis of semolina are summarized in Table 2. The average particle size of semolina is between 500 and 600 μm. Moisture content is 11.40%. The moisture of samples remained within the safety limits ≤ 14.5%, (AOJ, 1997). Semolina particles have a bright yellow color, with a lightness L_+ value 75.71. The a_+ value (red-green) and b_+ value (yellow-blue) were −0.27 and 26.82, respectively, as shown in Table 2. Semolina color is an important quality attribute in the food industries and it influences consumer's choices and preferences. The final color is the result of the balance between yellow and brown components in semolina. Carotenoid pigments and lipoxygenase (LOX) enzyme are mainly involved in yellowness, whereas peroxidase (POD) and ash affect brown hue (Borrelli et al., 2008). The L_+ and b_+ values are considered more important as color attributes at higher levels (Boudalia et al., 2016). In this study, the L_+ and b_+ values were higher and this contributed to the brightness and yellowness of the

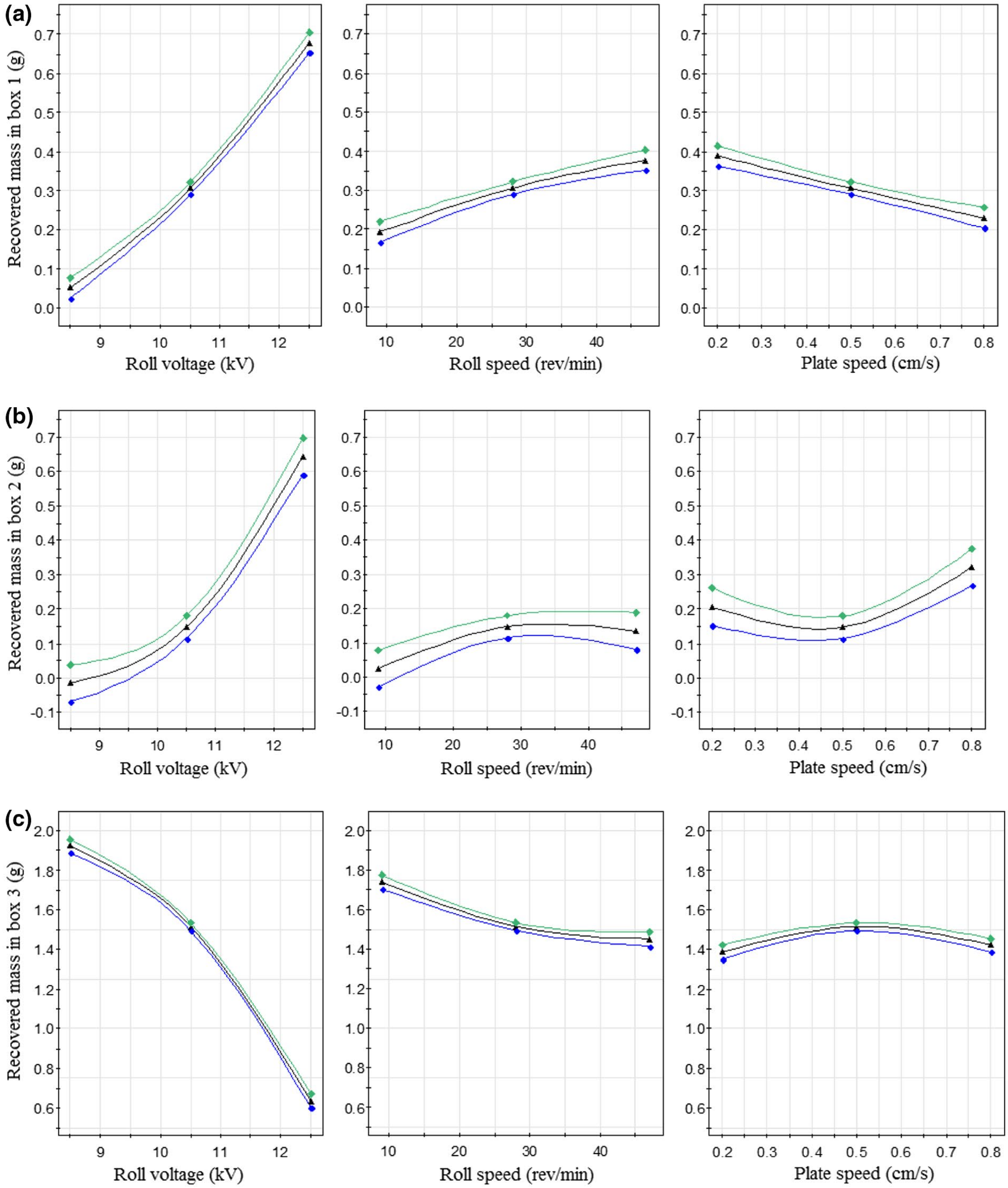

FIGURE 12 MODDE-predicted recovered mass in (a) box 1, (b) box 2, and (c) box 3, as a function of the applied voltage U (kV), the roll speed n (rpm) and the plate speed v (cm/s). In each case, the other variable is maintained constant and equal to its central value $U = 10.5$ kV, $n = 28$ rpm, and $v = 0.5$ cm/s. The upper and lower curves on each graph indicate the limits of the 95% confidence level interval

semolina samples. Also, as ash content reflects the purity of the semolina. Semolina with high ash content generally will have a high speck count. Bran, weed seeds, and soil are high in ash. For this reason, ash is commonly used in semolina specifications to ensure low contamination (Huin, 2006). The semolina samples presented a good proportion of starchy endosperm and are characterized by a low value of its ash content (1.13 ± 0.02%). Consequently, the samples have a medium purity. According to the Algerian Official Journal (AOJ, 1997), the results of ash analysis (Table 2) of the obtained fraction of semolina is classified: durum wheat ordinary semolina from the second grade.

Based on these results, it can be concluded that semolina fraction recovered from wheat bran residues was found to have an acceptable quality grade in the food industry. Therefore, the separation

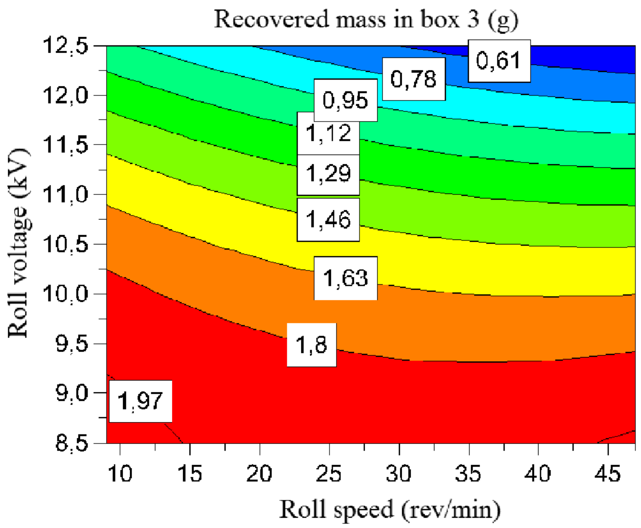

FIGURE 13 MODDE-computed equal response contours of recovered mass in box 3

TABLE 2 Physical and chemical analyses of semolina fraction

Granularity (μm)	Moisture content (%)	Ash content (%)	Color		
			L_+ value	a_+ value	b_+ value
500–600	11.40	1.13 ± 0.02	75.71	−0.27	26.82

process can be considered optimal. The excellent obtained results prove the effectiveness of the wheat bran recycling proposed procedure based on the association between wheat bran grinding and electrostatic separation. The proposed technique allows enhancing the extraction of semolina through the recovery of residuals in bran particles, until 50% from the treated wheat bran weight.

4 | CONCLUSION

The paper was devoted to the improvement of the extraction rate of semolina through recovering residual endosperm attached to wheat bran obtained after traditional milling.

- The mechanical abrasion and then electro-separation of the wheat bran has allowed a recovery of 50% of semolina from the initially treated mass, with only 1.1% ash content as quality.
- Through the lab-made abrasive device it was possible to detach significant quantities of endosperms still adhering to the bran layers after traditional milling. The particles of the semolina obtained after separation has identical physical dimensions to traditionally obtained particles after milling.
- The electrically conductive behavior of the wheat bran allowed the use of an electrostatic induction mechanism during separation.
- Three components were recovered after wheat bran treatment: semolina, fine bran, and relatively big bran. The electro-separation is a very interesting way to separate fine components where sieving is not possible.

ACKNOWLEDGMENT

The authors are grateful to engineers at the quality control laboratory at Amor BenAmor group and Biology lab at Guelma University for their kind help in realizing analysis and microscope observations.

CONFLICT OF INTEREST

The authors have declared no conflicts of interest for this article.

AUTHOR CONTRIBUTIONS

Conceptualization; Formal analysis; Investigation; Methodology; Visualization; Writing-original draft: kahaleras. *Formal analysis; Investigation; Methodology; Software; Writing-review & editing*: Remadnia. *Methodology; Project administration; Supervision; Validation; Writing-review & editing*: Kachi. *Formal analysis; Writing-review & editing*: Nadjem.

ORCID

Miloud Kachi https://orcid.org/0000-0002-5074-2681

REFERENCES

Algerian Official Journal. (1997, 20 Août). Arrêté interministériel du 25 Mai 1997 relatif aux spécifications techniques des semoules de blé dur et aux conditions et modalités de leur étiquetage. *Numéro.*, *55*, 15–16.(in French).

Barakat, A., & Mayer-Laigle, C. (2017). Electrostatic separation as an entry into environmentally eco-friendly dry biorefining of plant materials. *Journal of Chemical Engineering & Process Technology*, *8*, 1–6. https://doi.org/10.4172/2157-7048.1000354

Borrelli, G. M., De Leonardis, A. M., Platani, C., & Troccoli, A. (2008). Distribution along durum wheat kernel of the components involved in semolina colour. *Journal of Cereal Science*, *48*, 494–502. https://doi.org/10.1016/j.jcs.2007.11.007

Boudalia, S., Mezroua, E. Y., Bousbia, A., Khaldi, M., Merabti, W., & Namoune, H. (2016). Evaluation of the stability of the physico-chemical properties and sensory qualities of farfalle pasta from the region of Guelma, Algeria. *Malaysian Journal of Nutrition*, *22*, 443–453.

Burton Rachel, A., & Fincher Geoffrey, B. (2014). Evolution and development of cell walls in cereal grains. *Frontiers in Plant Science*, *5*, 1–15. https://doi.org/10.3389/fpls.2014.00456

Chubb, J. N. (2010). *An introduction to electrostatic measurements*. Nova Publishers.

Eriksson, L., Johansson, E., Kettaneh-Wold, N., Wikström, C., & Wold, S. (2008). *Design of experiments: Principles and applications*. Umetrics Academy.

Frigon, N. L., & Mathews, D. (1996). *Practical guide to experimental design*. Wiley.

Hemery, Y., Holopainen, U., Lampi, A. M., Lehtinen, P., Nurmi, T., Piironen, V., Edelmann, M., & Rouau, X. (2011). Potential of dry fractionation of wheat bran for the development of food ingredients, part II: Electrostatic separation of particles. *Journal of Cereal Science*, *53*, 9–18. https://doi.org/10.1016/j.jcs.2010.06.014

Hill, V. (2014). *A Kaizen approach to food safety: Quality management in the value chain from wheat to bread*. Springer International Publishing.

Hossain, K., Ulven, C., Glover, K., Ghavami, F., Simsek, S., Alamri, M. S., Kumar, A., & Mergoum, M. (2013). Interdependence of cultivar and environment on fiber composition in wheat bran. *Australian Journal of Crop Science*, *7*, 525–531.

Hourston, J. E., Ignatz, M., Reith, M., Leubner-Metzger, G., & Steinbrecher, T. (2017). Biomechanical properties of wheat grains: The implications on milling. *Journal of the Royal Society Interface*, *14*, 1–12. https://doi.org/10.1098/rsif.2016.0828

Huin, Y. H. (2006). *Handbook of food science, technology, and engineering*. CRC Press, Taylor & Francis Group.

Hutkins Robert, W. (2019). *Microbiology and technology of fermented foods*, 2nd ed. IFT Press, Wiley-Blackwell.

Kachi, M., Nemamcha, M., Tabti, B., & Dascalescu, L. (2011). Comparison between three measurement methods for characterizing the charge state of granular insulating materials. *Journal of Electrostatics*, *69*, 394–400. https://doi.org/10.1016/j.elstat.2011.05.002

Kdidi, S., Vaca-Medina, G., Peydecastaing, J., Oukarroum, A., Fayoud, N., & Barakat, A. (2019). Electrostatic separation for sustainable production of rapeseed oil cake protein concentrate: Effect of mechanical disruption on protein and lignocellulosic fiber separation. *Powder Technology*, *344*, 10–16. https://doi.org/10.1016/j.powtec.2018.11.107

Kulp, K. (2000). *Handbook of cereal science and technology*, 2nd ed. CRC Press.

Laguna, O., Barakat, A., Alhamada, H., Durand, E., Baréa, B., Fine, F., Villeneuve, P., Citeau, M., Dauguet, S., & Lecomte, J. (2018). Production of proteins and phenolic compounds enriched fractions from rapeseed and sunflower meals by dry fractionation processes. *Industrial Crops & Products*, *118*, 160–172. https://doi.org/10.1016/j.indcrop.2018.03.045

Onipe, O. O., Jideani, A. I. O., & Beswa, D. (2015). Composition and functionality of wheat bran and its application in some cereal food products. *International Journal of Food Science and Technology*, *50*, 2509–2518. https://doi.org/10.1111/ijfs.12935

Rajaonarivony, R. K., Rouau, X., Dascalescu, L., & Mayer-Laigle, C. (2017). Electrostatic separation of mineral and vegetal powders with a custom built corona separator: Application to biorefinery of rice husk. *EPJ Web of Conferences*, *140*, 1–4. https://doi.org/10.1051/epjconf/201714013020

Remadnia, M., Kachi, M., Messal, S., Oprean, A., Rouau, X., & Dascalescu, L. (2014). Electrostatic separation of peeling and gluten from finely ground wheat grains. *Particulate Science and Technology*, *32*, 608–615. https://doi.org/10.1080/02726351.2014.943379

Remadnia, M., Nemamcha, M., Herous, L., & Dascalescu, L. (2011). Decay of electric potential at the surface of corona charged uniform layers of HIPS granules. *IEEE Transactions of Dielectrics and Insulating Materials*, *18*, 579–587. https://doi.org/10.1109/TDEI.2011.5739464

Samaan, J. (2007). *Characterisation of grain quality of Syrian durum wheat genotypes affecting milling performance and end-use quality*. (PhD thesis)University of Plymouth.

Surget, A., & Barron, C. (2005). Histologie du grain de blé. *Industrie Des Céréales*, *145*, 3–7.

Umetrics. (2006). *MODDE 8.0 - User guide and tutorial.* : Author.

Wang, J., de Wit, M., Schutyser, M. A. I., & Boom, R. M. (2014). Analysis of electrostatic powder charging for fractionation of foods. *Innovative Food Science & Emerging Technologies*, *26*, 360–365. https://doi.org/10.1016/j.ifset.2014.06.011

Wang, J., Smits, E., Boom, R. M., & Schutyser, M. A. I. (2015). Arabinoxylans concentrates from wheat bran by electrostatic separation. *Journal of Food Engineering*, *155*, 29–36. https://doi.org/10.1016/j.jfoodeng.2015.01.008

SUPPORTING INFORMATION

Additional Supporting Information may be found online in the Supporting Information section.

How to cite this article: Kahaleras M, Remadnia M, Kachi M, Nadjem A. Semolina extraction from wheat bran using an electro-separation process. *J Food Process Preserv*. 2021;45:e15352. https://doi.org/10.1111/jfpp.15352